

Survival of Planets Around Shrinking Stellar Binaries

Diego J. Muñoz* and Dong Lai

Center for Space Research, Department of Astronomy, Cornell University, Ithaca, NY 14853, USA

2 March 2024

The discovery of transiting circumbinary planets by the *Kepler* mission suggests that planets can form efficiently around binary stars. None of the stellar binaries currently known to host planets has a period shorter than 7 days, despite the large number of eclipsing binaries found in the Kepler target list with periods shorter than a few days. These compact binaries are believed to have evolved from wider orbits into their current configurations via the so-called Lidov-Kozai migration mechanism, in which gravitational perturbations from a distant tertiary companion induce large-amplitude eccentricity oscillations in the binary, followed by orbital decay and circularization due to tidal dissipation in the stars. Here we explore the orbital evolution of planets around binaries undergoing orbital decay by this mechanism. We show that planets may survive and become misaligned from their host binary, or may develop erratic behavior in eccentricity, resulting in their consumption by the stars or ejection from the system as the binary decays. Our results suggest that circumbinary planets around compact binaries could still exist, and we offer predictions as to what their orbital configurations should be like.

planet dynamics and stability — close stellar binaries — multiple stellar systems

To date, the *Kepler* spacecraft has discovered eight binary star systems harboring ten transiting circumbinary planets Doyle et al. (2011); Welsh et al. (2012); Orosz et al. (2012,?); Schwamb et al. (2013); Kostov et al. (2013, 2014); Welsh et al. (2014). These systems have binary periods ranging from 7.5 to ~ 41 days, while the planet periods range from ~ 50 to ~ 250 days. Remarkably, no transiting planets have been found around more compact stellar binaries, those with orbital periods of $\lesssim 5$ days. Planets around such compact binaries, if orbiting in near coplanarity, should have transited several times over the lifetime of the *Kepler* mission. However, the shortest period binary hosting a planet is Kepler-47(AB) with 7.44 days, despite the fact that nearly 50% of the eclipsing binaries in the early quarters of Kepler data have periods shorter than 3 days Slawson et al. (2011). Thus, the apparent absence of planets around short-period binaries is statistically significant [e.g., Armstrong et al. (2014)].

It is widely believed that short-period binaries ($\lesssim 5$ days) are not primordial, but have evolved from a wider configurations via Lidov-Kozai (LK) cycles Lidov (1962); Kozai (1962) with tidal friction Mazeh & Shaham (1979); Eggleton & Kiseleva-Eggleton (2001); Fabrycky & Tremaine (2007). This “LK+tide” mechanism requires an external tertiary companion at high inclination to excite the inner binary eccentricity such that tidal dissipation becomes important at pericenter, eventually leading to orbital decay and circularization. A rough transition at an orbital period of 6 days has

been identified as the separation between “primordial” and “tidally evolved” binaries Fabrycky & Tremaine (2007). Indeed, binaries with periods shorter than this threshold are known to have very high tertiary companion fractions [of up to 96% for periods < 3 days; see Tokovinin et al. (2006)], supporting the idea that three-body interactions have played a major role in their formation.

In synthetic population studies Fabrycky & Tremaine (2007), stellar binaries with periods shorter than ~ 5 days evolved from binaries with original periods of ~ 100 days. Interestingly, it is around binaries with periods $\lesssim 100$ days that transiting planets have been detected. It is thus plausible that current compact binaries with a tertiary companion may have once been primordial hosts to planets like those detected by *Kepler*.

In this work, we study the evolution and survival of planets around stellar binaries undergoing orbital shrinkage via the “LK+tide” mechanism. We follow the secular evolution of the planet until binary circularization is reached and binary separation is shrunk by an order of magnitude. We show that the tertiary companion can play a major role in misaligning and/or destabilizing the planet as the binary shrinks.

A PLANET INSIDE A STELLAR TRIPLE

Consider a planet orbiting a circular stellar binary of total mass $M_{\text{in}} = m_0 + m_1$ and semimajor axis a_{in} ; the binary is a member of a hierarchical triple, in which the binary and an outer companion of mass M_{out} orbit each other with a semimajor axis $a_{\text{out}} \gg a_{\text{in}}$.

* E-mail: dmunoz@astro.cornell.edu

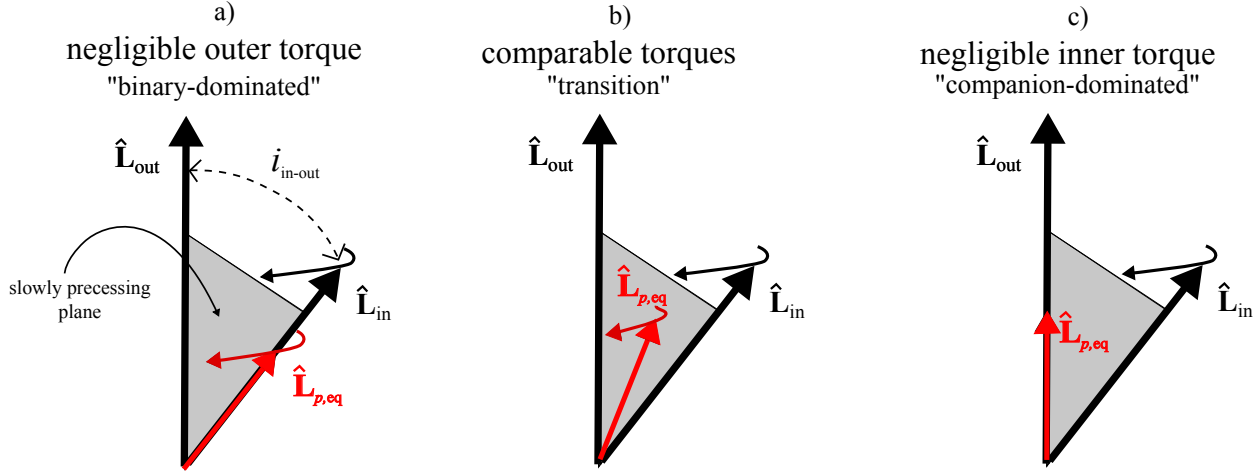
Steady-state planetary orientation $\hat{\mathbf{L}}_{p,\text{eq}}$ for a circular, precessing inner binary

Figure 1. The planet’s angular momentum orientation $\hat{\mathbf{L}}_p$ precesses around the equilibrium solution $\hat{\mathbf{L}}_{p,\text{eq}}$ (red vector), which is obtained from balancing the torques acting on the planet due to the inner binary and the outer companion. The limiting cases are (a) $\hat{\mathbf{L}}_{p,\text{eq}} \parallel \hat{\mathbf{L}}_{\text{in}}$ (planet at small distance a_p from the inner binary, where outer torque is negligible) and (c) $\hat{\mathbf{L}}_{p,\text{eq}} \parallel \hat{\mathbf{L}}_{\text{out}}$ (at large distance, where the inner torque is negligible), while (b) represents the intermediate cases where the two torques have comparable magnitudes. The continuous variation of $\hat{\mathbf{L}}_{p,\text{eq}}$ with a_p (always coplanar with $\hat{\mathbf{L}}_{\text{in}}$ and $\hat{\mathbf{L}}_{\text{out}}$) going from (a) to (b) to (c) defines the so-called “Laplace surface”. When the inner binary axis $\hat{\mathbf{L}}_{\text{in}}$ precesses slowly around $\hat{\mathbf{L}}_{\text{out}}$ by the action of the outer companion, $\hat{\mathbf{L}}_{p,\text{eq}}$ follows adiabatically and stays coplanar with $\hat{\mathbf{L}}_{\text{in}}$ and $\hat{\mathbf{L}}_{\text{out}}$. If the torque from the inner binary is slowly decreased in time, (e.g., due to orbital decay), $\hat{\mathbf{L}}_{p,\text{eq}}$ not only will precess around $\hat{\mathbf{L}}_{\text{out}}$, but will also change its inclination, going smoothly from regime (a) to regime (c).

The secular (long term) gravitational perturbations exerted on the planetary orbit from the quadrupole potential associated¹ with the inner binary and that from the outer companion cause the two vectors that determine the orbital properties of the planet, the angular momentum direction $\hat{\mathbf{L}}_p$ and the eccentricity vector \mathbf{e}_p , to evolve in time. The inner binary tends to make $\hat{\mathbf{L}}_p$ precess around $\hat{\mathbf{L}}_{\text{in}}$, the unit vector along the inner binary’s angular momentum, at a rate approximately given by

$$\Omega_{p\text{-in}} \equiv \frac{1}{2} n_p \left(\frac{\mu_{\text{in}}}{M_{\text{in}}} \right) \left(\frac{a_{\text{in}}}{a_p} \right)^2, \quad (1)$$

where a_p is the semi-major axis of the planet, $n_p = \sqrt{\mathcal{G}M_{\text{in}}/a_p^3}$ is the planet’s mean motion frequency (assumed to be on a circular orbit), and $\mu_{\text{in}} = m_0 m_1 / M_{\text{in}}$ is the reduced mass of the inner stellar pair. Similarly, the outer companion of mass M_{out} tends to make $\hat{\mathbf{L}}_p$ precess around $\hat{\mathbf{L}}_{\text{out}}$ at a rate approximately given by²,

$$\Omega_{p\text{-out}} \equiv n_p \left(\frac{M_{\text{out}}}{M_{\text{in}}} \right) \left(\frac{a_p}{a_{\text{out}}} \right)^3. \quad (2)$$

In general, when the torques from the inner binary and the outer companion are of comparable magnitude, $\hat{\mathbf{L}}_p$ will precess around an intermediate vector $\hat{\mathbf{L}}_{p,\text{eq}}$, which corresponds to the equilibrium solution (i.e., $d\hat{\mathbf{L}}_p/dt = 0$) of the planet’s orbit under the two torques. For a general mutual inclination angle $i_{\text{in-out}}$ between the inner and outer orbits (where $\cos i_{\text{in-out}} = \hat{\mathbf{L}}_{\text{in}} \cdot \hat{\mathbf{L}}_{\text{out}}$), the equilibrium inclination of the planet (the so-called “Laplace surface”; see Tremaine et al. (2009); Tamayo et al. (2013)), can be

found as a function of its semimajor axis, for which $\hat{\mathbf{L}}_{p,\text{eq}}$ is always coplanar with $\hat{\mathbf{L}}_{\text{in}}$ and $\hat{\mathbf{L}}_{\text{out}}$, with limiting states corresponding to alignment with the inner binary (i.e., $\hat{\mathbf{L}}_{p,\text{eq}} \parallel \hat{\mathbf{L}}_{\text{in}}$) at small a_p , and alignment with the outer companion (i.e., $\hat{\mathbf{L}}_{p,\text{eq}} \parallel \hat{\mathbf{L}}_{\text{out}}$) at large a_p . The transition between these two orientations happens rapidly at the so-called “Laplace radius” r_L , obtained by setting $\Omega_{p,\text{out}} = \Omega_{p,\text{in}}$, and is given by

$$r_L = \left(\frac{\mu_{\text{in}}}{2M_{\text{out}}} a_{\text{in}}^2 a_{\text{out}}^3 \right)^{1/5}. \quad (3)$$

Fig. 1 illustrates the three regimes of the planet’s equilibrium orientation: (a) $\Omega_{p\text{-in}} \gg \Omega_{p\text{-out}}$ (binary-dominated regime, or $a_p \ll r_L$); (b) $\Omega_{p\text{-out}} \sim \Omega_{p\text{-in}}$ (transition regime, or $a_p \sim r_L$); and (c) $\Omega_{p\text{-out}} \gg \Omega_{p\text{-in}}$ (companion-dominated regime, or $a_p \gg r_L$).

In general, however, the vector $\hat{\mathbf{L}}_{\text{in}}$ is not fixed in space, but slowly precesses around $\hat{\mathbf{L}}_{\text{out}}$, owing to the torque from the outer companion³. This means that the plane normal to $\hat{\mathbf{L}}_{\text{in}} \times \hat{\mathbf{L}}_{\text{out}}$, where the equilibrium orientation vector $\hat{\mathbf{L}}_{p,\text{eq}}$ lives, is slowly rotating (Fig. 1). This rotation rate is of order

$$\Omega_{\text{in-out}} \equiv n_{\text{in}} \left(\frac{M_{\text{out}}}{M_{\text{in}}} \right) \left(\frac{a_{\text{in}}}{a_{\text{out}}} \right)^3, \quad (4)$$

where $n_{\text{in}} = \sqrt{\mathcal{G}M_{\text{in}}/a_{\text{in}}^3}$ is the mean motion of the inner binary. Note that $\Omega_{p\text{-out}}/\Omega_{\text{in-out}} = (a_p/a_{\text{in}})^{3/2} \gg 1$ in the companion-dominated regime, and $\Omega_{p\text{-in}}/\Omega_{\text{in-out}} = (\Omega_{p\text{-in}}/\Omega_{p\text{-out}})(a_p/a_{\text{in}})^{3/2} = (r_L/a_p)^5 (a_p/a_{\text{in}})^{3/2} \gg 1$ in the binary-dominated regime. This means that the precession of $\hat{\mathbf{L}}_{\text{in}}$ is always slow enough for $\hat{\mathbf{L}}_p$ to adiabatically follow. In other words, the classical Laplace equilibrium formalism remains valid in the

¹ If the inner binary has an equal-mass ratio and the outer companion has zero eccentricity, the octupole-order terms in the potential vanish exactly.

² Although we assume a circular outer companion here, the eccentricity of the outer orbit e_{out} can be taken into account by replace a_{out} with $a_{\text{out}} \sqrt{1 - e_{\text{out}}^2}$.

³ Strictly speaking, both $\hat{\mathbf{L}}_{\text{in}}$ and $\hat{\mathbf{L}}_{\text{out}}$ precess around the *total* angular momentum vector of the system; however, for the hierarchical configurations presented here, the outer orbit contains most of the angular momentum of the system, implying that $\hat{\mathbf{L}}_{\text{out}}$ is approximately fixed in space.

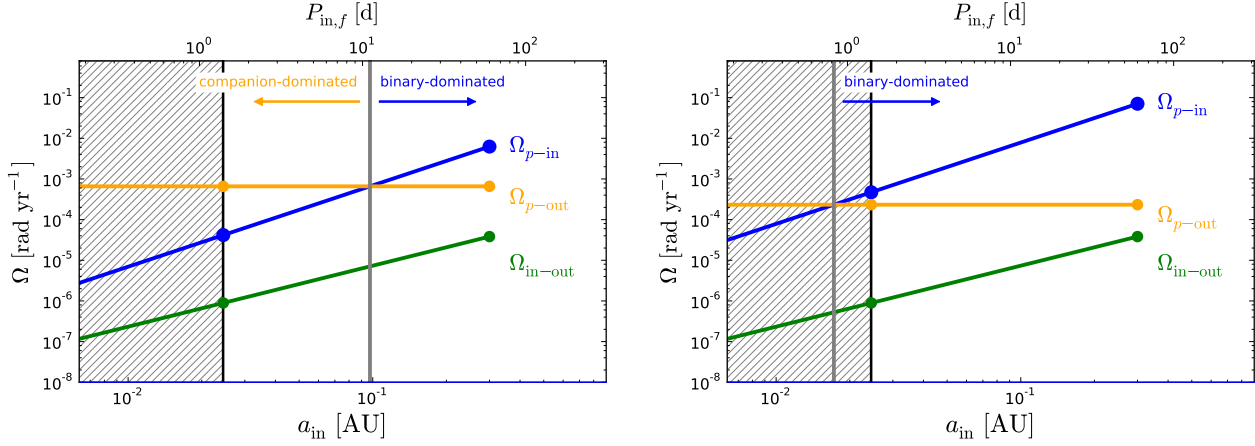


Figure 2. The three relevant precession frequencies (Ω_{p-in} , Ω_{p-out} and Ω_{in-out}) as a function of the shrinking binary semimajor axis a_{in} . The binary starts at semimajor axis $a_{in,0} = 0.3$ AU and circularizes at $a_{in,f} = 0.024$ AU (vertical black line). The other parameters are $M_{in} = M_{out} = 1M_{\odot}$, $\mu_{in} = 0.25$, $a_{out} = 30$ AU and $e_{out} = 0$. The left panel shows the case with $a_p = 2$ AU, and the right panel one with $a_p = 1$ AU. On the left panel, a_{in} crosses $a_{in,L} = 0.097$ AU (thick vertical gray line), during orbital decay, then the planet transitions from the binary-dominated regime into the companion-dominated regime. On the right panel, $a_{in,f} > a_{in,L} = 0.017$ AU and the planet will stay in the binary-dominated regime throughout the binary orbital decay. Note, that in this example, $a_p = 1$ AU is very close to the initial binary, and dynamical instabilities (not captured by secular calculations) might make the survival of these planets difficult during the early Lidov-Kozai cycles of the binary.

frame corotating with $\hat{\mathbf{L}}_{in}$, and the three vectors $\hat{\mathbf{L}}_{in}$, $\hat{\mathbf{L}}_{out}$ and $\hat{\mathbf{L}}_{p,eq}$ remain coplanar at all times. Since the evolution is adiabatic, if $\hat{\mathbf{L}}_p$ starts parallel to $\hat{\mathbf{L}}_{p,eq}$, it will remain parallel to the evolving $\hat{\mathbf{L}}_{p,eq}$ at later times, provided that this equilibrium orientation is a stable solution Tremaine et al. (2009).

As studied by Tremaine et al. (2009), when $i_{in-out} > 69^\circ$, circular orbits on the Laplace surface are unstable to linear perturbations in the planet’s eccentricity vector \mathbf{e}_p vector for a range of a_p around r_L . This instability manifests itself as an exponential growth of e_p , until non-linear effects come into play, resulting in erratic behavior in both inclination and eccentricity. This means that above this critical value of i_{in-out} , planets cannot be placed at $a_p \sim r_L$, since the resulting high eccentricities could bring them too close to the binary, at which point they may collide with the central stars or be ejected from the system [e.g., Holman & Wiegert (1999)].

Now consider what will happen to the planet’s orbit as the inner binary undergoes orbital decay. For simplicity, let us assume that the binary remains circular during this process, and that the angle i_{in-out} remains unchanged. Since orbital decay takes place over a time scale t_{decay} much longer than the other relevant time scales ($1/\Omega_{p-in}$, $1/\Omega_{p-out}$ and $1/\Omega_{in-out}$), the system will evolve adiabatically. Thus, if the planet initially resides in the binary-dominated regime ($\Omega_{p-in} \gg \Omega_{p-out}$, $a_p \ll r_L$), and lives on the Laplace surface ($\hat{\mathbf{L}}_p \parallel \hat{\mathbf{L}}_{p,eq}$), it will transition to the companion-dominated regime ($\Omega_{p-in} \ll \Omega_{p-out}$, $a_p \gg r_L$) through the intermediate stage ($\Omega_{p-in} \sim \Omega_{p-out}$), as the inner binary’s semi-major axis a_{in} decreases. For a given value of a_p , the transition occurs when a_{in} passes through a critical (“Laplace”) value,

$$a_{in,L} \equiv 0.017 \left(\frac{M_{out}}{4\mu_{in}} \right)^{1/2} \left(\frac{a_p}{1 \text{ AU}} \right)^{5/2} \left(\frac{a_{out}}{30 \text{ AU}} \right)^{-3/2} \text{ AU} \quad (5)$$

obtained by replacing $r_L = a_p$ in Eq. 3 and solving for a_{in} . If the transition region ($a_p \sim r_L$) is stable, we expect the planet’s orbit to evolve smoothly following the Laplace surface [i.e., (a)→(b)→(c) in Fig. 1]. For $i_{in-out} > 69^\circ$, however, the planet will encounter

an instability when $a_p \sim r_L$, and may undergo erratic evolution, which may result in the planet being destroyed or ejected.

In the “LK+tide” scenario for the formation of compact binaries, the final inner binary separation $a_{in,f}$ depends on the properties of the outer companion (M_{out} , a_{out} and the initial inclination i_{in-out}) as well as on the short-range force effects between the inner binary members Fabrycky & Tremaine (2007). Thus, for a given stellar triple configuration, the inner binary may or may not reach down to $a_{in,L}$, depending on the value of a_p (see Fig. 2). If $a_{in,f} > a_{in,L}$, or equivalently, if

$$a_p < 1.26 \left(\frac{M_{out}}{4\mu_{in}} \right)^{-1/5} \left(\frac{a_{out}}{30 \text{ AU}} \right)^{3/5} \left(\frac{a_{in,f}}{0.03 \text{ AU}} \right)^{2/5} \text{ AU}, \quad (6)$$

the planet will never cross the intermediate regime ($a_p \sim r_L$), and it will thus remain “safe” (stable), regardless of the inclination i_{in-out} , surviving the orbital decay of its host binary.

EVOLUTION OF PLANETARY ORBITS AROUND BINARIES UNDERGOING LIDOV-KOZAI CYCLES WITH TIDAL FRICTION

The greatest caveat to the application of classical Laplace equilibrium is that the inner binary does not remain circular during orbital decay. Indeed, in the “LK+tide” mechanism Eggleton & Kiseleva-Eggleton (2001); Fabrycky & Tremaine (2007) the inner binary exhibits large oscillations in inclination and eccentricity under the influence of the external stellar companion. Thus the binary axis $\hat{\mathbf{L}}_{in}$ not only precesses around $\hat{\mathbf{L}}_{out}$, but also undergoes nutation. The variation of the inner binary’s eccentricity vector \mathbf{e}_{in} also affects the torque on the circumbinary planet.

To track the evolution of the planet’s orbit during the LK oscillations and orbital decay of the inner binary, we solve numerically the secular equations of ⁴ of the planet’s eccentricity vector

⁴ The secular equations of motion govern the evolution of the orbital elements instead of the position and velocity of individual bodies.

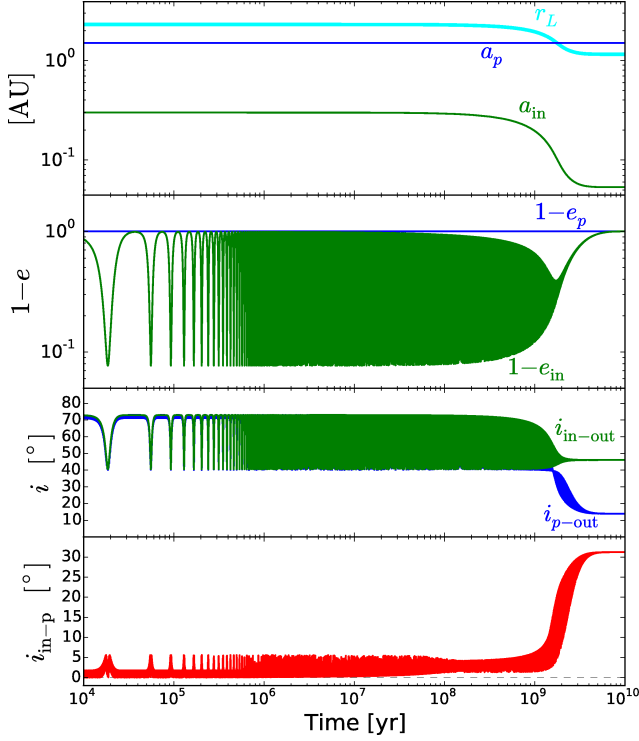


Figure 3. An example of the coupled evolution of an inner binary within a stellar triple ($m_0 = m_1 = 0.5M_\odot$, $M_{\text{out}} = 1M_\odot$, $a_{\text{out}} = 18$ AU and initial $a_{\text{in},0} = 0.3$ AU and $i_{\text{in-out},0} = 73^\circ$) plus a planet with semimajor axis $a_p = 1.5$ AU. The different panels show: (top) binary semimajor axis a_{in} (green) and planet semimajor axis a_p (blue) and the Laplace radius r_L (cyan); (top middle) eccentricity of the binary e_{in} (green) and eccentricity of the planet e_p (blue); (top bottom) inclination of the binary $i_{\text{in-out}}$ (green) and inclination of the planet $i_{p\text{-out}}$ (blue) with respect to the outer companion; and (bottom) mutual inclination between the planet and the binary $i_{p\text{-in}}$. The eccentricity and inclination of the binary exhibit LK cycles for about 10% of the integration time, until short-range forces arrest these oscillations (freezing e_{in} at high values), at which point a slow phase of orbital decay takes place. The planet starts in the binary-dominated regime ($a_p/r_{L,0} = 0.65$). Its inclination $i_{p\text{-out}}$ follows closely that of the inner binary $i_{\text{in-out}}$ until r_L crosses a_p (note that the definition of r_L in Eq. 3 does not take into account the eccentricity of the inner binary e_{in}), at which point these two inclination angles decouple from each other. The planet ends in the companion dominated regime ($a_p/r_{L,f} = 1.3$), and its inclination with respect to the binary $i_{p\text{-in}}$ eventually settles into a constant value of $\sim 32^\circ$.

\mathbf{e}_p and angular momentum vector axis $\hat{\mathbf{L}}_p$ (see Supplementary Information), along with the evolution equations of the stellar triple. We use the formalism of Eggleton et al. (1998) to follow the inner binary's orbit and parametrize the stellar tidal dissipation rate using the weak friction model with constant tidal lag time. In the following, we focus on a few representative examples and discuss the general behavior for the evolution of the four-body system.

Fig. 3 depicts a system where the stellar triple has parameters $m_0 = m_1 = 0.5M_\odot$, $M_{\text{out}} = 1M_\odot$, $a_{\text{out}} = 18$ AU and $e_{\text{out}} = 0$ and initial values $a_{\text{in},0} = 0.3$ AU and $i_{\text{in-out},0} = 73^\circ$, and where the planet is initialized on a circular orbit at $a_p = 1.5$ AU with $\hat{\mathbf{L}}_p$ aligned with $\hat{\mathbf{L}}_{\text{in}}$. The parameters for the inner binary and the planet are chosen to roughly correspond to the discovered *Kepler* systems. The parameters for the outer orbit are chosen to ensure that LK cycles are not suppressed by short-range forces and to guarantee the efficient orbital decay of the inner

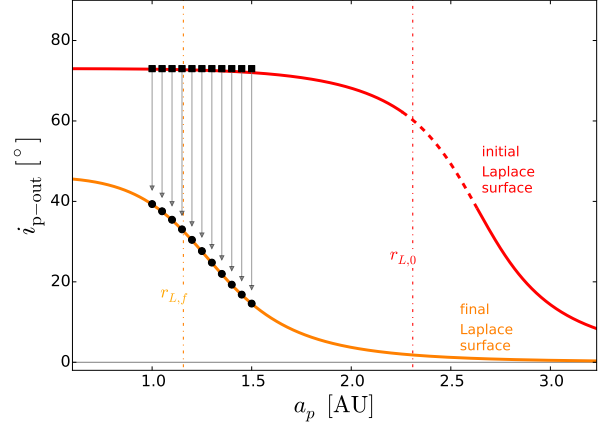


Figure 4. Classical Laplace equilibrium surface (valid for $e_{\text{in}} = 0$) at the beginning (red curve) and after circularization of the inner binary (orange curve) for the triple configuration of Fig. 3 ($m_0 = m_1 = 0.5M_\odot$, $M_{\text{out}} = 1M_\odot$, $a_{\text{in},0} = 0.3$ AU, $i_{\text{in-out},0} = 73^\circ$, $a_{\text{in},f} = 0.053$ AU, $i_{\text{in-out},f} = 46.1^\circ$ and $a_{\text{out}} = 18$ AU). The dotted portion of the red line indicates the range of radii at which the equilibrium surface is unstable (Tremaine et al. 2009). The final Laplace surface is stable for all a_p since $i_{p\text{-out},f} < 60^\circ$. The vertical dash-dotted lines indicate the Laplace radii at the beginning ($r_{L,0}$) and end ($r_{L,f}$) of the binary orbital evolution. For the different values of a_p , vertical arrows connect the initial and final states, representing the evolution of the planet's inclination obtained from the numerical calculations. In each case, the planet orientation is initially aligned with the local Laplace surface (or approximately aligned with the binary for $a_p \lesssim 1.5$ AU); after the inner binary has decayed and circularized, the planet inclination settles into a value coincident with final Laplace surface. Note that, for illustrative purposes, we include values of a_p down to 1 AU; however, dynamical stability dictates that only planets outside $a_p \sim 4a_{\text{in}} \sim 1.2$ AU (when $e_{\text{in}} \sim 1$; Holman & Wiegert 1999) should survive the early LK cycles of the inner binary.

binary Fabrycky & Tremaine (2007). In our calculations, the octupole term in the potential has been ignored in the evolution equations of the planet and the inner binary, a justified simplification since $m_0 = m_1$ and $e_{\text{out}} = 0$. The inner binary experiences LK oscillations and circularizes within a Hubble time provided that enough tidal dissipation is present in the stars. The final (circularization) semimajor axis is $a_{\text{in},f} = 0.053$ AU (corresponding to an orbital period of 4.5 days). In this example, the planet initially resides in the binary-dominated regime, with $\Omega_{p\text{-in}}/\Omega_{p\text{-out}} \approx 65(a_p/\text{AU})^{-5} \approx 8.6$, and $a_p/r_{L,0} \approx 0.65$. After the inner binary has circularized, the planet lies in the companion-dominated regime, with $\Omega_{p\text{-in}}/\Omega_{p\text{-out}} \approx 0.27$ and $a_p/r_{L,f} \approx 1.3$. We see that the planet remains on a circular orbit throughout its entire evolution, despite the large variations in e_{in} during the LK cycles. The longitude of nodes of the planet (not shown in the figure) closely follows that of the inner binary during the early LK cycles and after circularization, implying that for a large fraction of the time $\hat{\mathbf{L}}_p$ is coplanar with $\hat{\mathbf{L}}_{\text{in}}$ and $\hat{\mathbf{L}}_{\text{out}}$. The planet's inclination $i_{p\text{-out}}$ also follows the binary inclination $i_{\text{in-out}}$ during the early stage of the LK cycles (third panel from top), but it decouples from the inner binary after a_{in} has started decreasing. At the end of the integration, when the binary has circularized, the binary and planet are misaligned by 32° (fourth panel) and the planet inclination has settled onto a steady-state value. This final value $i_{p\text{-out}} \simeq 14^\circ$ agrees with the equilibrium value of the end-state Laplace surface (with $a_{\text{in},f} = 0.053$ AU and $i_{\text{in-out},f} = 46^\circ$) evaluated at $a_p = 1.5$ AU.

We have carried out calculations for a range of values of a_p for the same stellar triple configuration of Fig. 3. The results

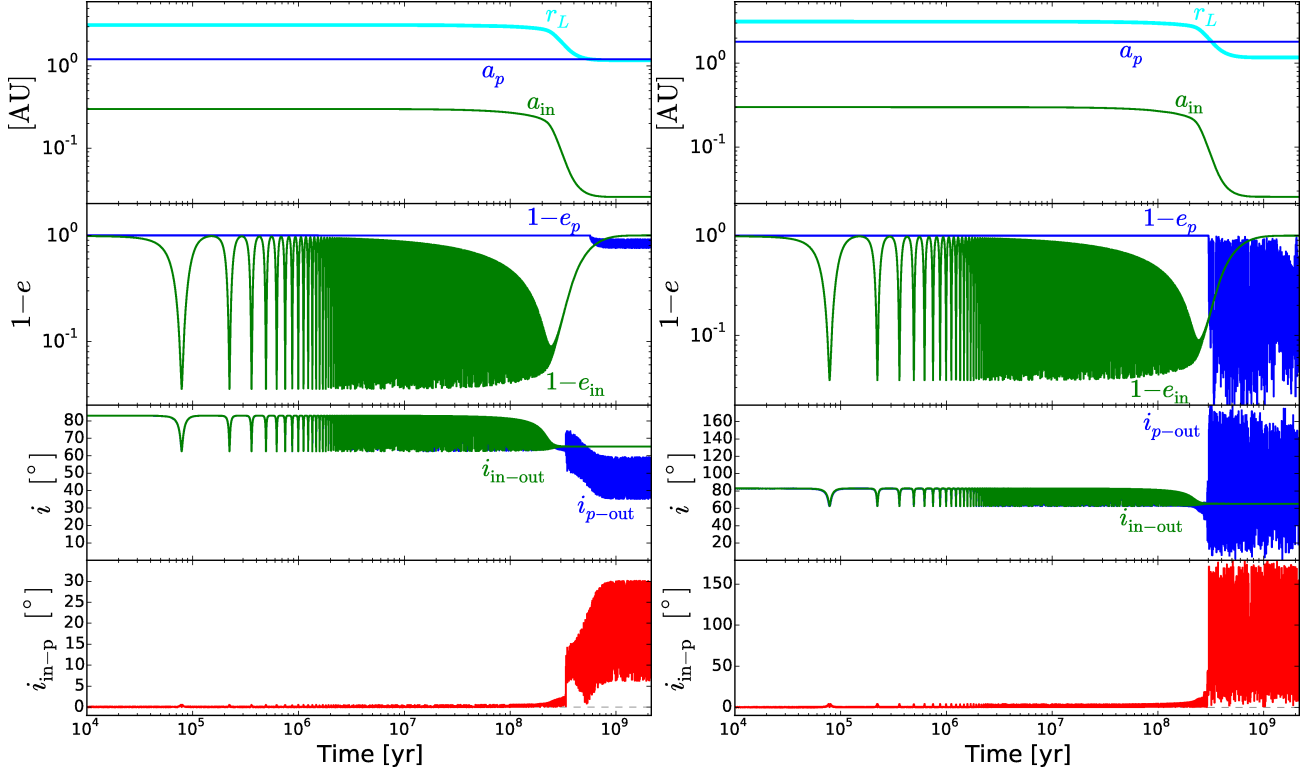


Figure 5. Similar to Fig. 3, but for a triple system that is initialized at a higher inclination $i_{\text{in-out},0} = 83^\circ$. The other parameters for the tare $a_{\text{in},0} = 0.3$ AU and $a_{\text{out}} = 30$ AU, with the same stellar masses as in Fig. 3. Two examples are shown: $a_p = 1.2$ AU (left panels) and $a_p = 1.8$ AU (right panels), both exhibiting quite different planetary evolution compared to Fig. 3. In the case of $a_p = 1.2$ AU, the planet starts with $a_p/r_{L,0} = 0.38$ and ends with $a_p/r_{L,f} = 1.02$; in the case of $a_p = 1.8$ AU, the planet starts with $a_p/r_{L,0} = 0.57$ and ends with $a_p/r_{L,f} = 1.54$.

of these calculations are summarized in Fig. 4, which shows the Laplace surfaces at the beginning and at the end of the evolution, when the inner binary is circular. In each case, the planet is initially aligned with the equilibrium orientation $\hat{\mathbf{L}}_{p,\text{eq}}$, which is in near alignment with the inner binary for $a_p \lesssim 1.5$ AU. We find that the planet’s inclination evolves smoothly for all these cases as the binary experiences LK oscillations and orbital decay. Despite the complexity of the “intermediate” states, in which the binary develops large eccentricities and the standard Laplace equilibrium is not well defined, we find that in the end, the planet’s inclination always lands on the final Laplace surface. Thus, these planets survive the orbital decay of the inner binary, but become inclined respect to it by an angle given by $i_{p\text{-in},f} = i_{\text{in-out},f} - i_{p\text{-out},f}$ (with $i_{\text{in-out},f} \approx 46^\circ$ for the parameters adopted in Figs. 3 and 4), where $i_{p\text{-out},f}$ matches the equilibrium inclination of the final Laplace surface. Since the Laplace equilibrium inclination angle decreases with increasing a_p , we predict that the angle $i_{p\text{-in}}$ of the planets that survive will increase monotonically with increasing a_p .

As noted before, when the mutual inclination $i_{\text{in-out}}$ between the inner circular binary and the external companion is greater than 69° , a portion of the Laplace surface is unstable Tremaine et al. (2009). In principle, a circumbinary planet may suffer a similar instability as a binary with large initial $i_{\text{in-out}}$ undergoes “LK+tide” orbital decay. In Fig. 5, we show two examples ($a_p = 1.2$ AU and $a_p = 1.8$ AU for the left and right panels, respectively) of planets within a stellar triple with $a_{\text{out}} = 30$ AU, $a_{\text{in},0} = 0.3$ AU, and $i_{\text{in-out},0} = 83^\circ$ (the other parameters are the same as in Fig. 3). At this initial inclination, the inner binary attains very high eccentricities and can circularize very efficiently (alter-

natively, it requires relatively small tidal dissipation in the stars to circularize within a Hubble time). The final binary separation is $a_{\text{in},f} = 2.55 \times 10^{-2}$ AU (period of 1.5 d) and the inclination angle freezes out at $i_{\text{in-out},f} = 65.3^\circ$. The behavior of the planets is markedly different from the one depicted in Fig. 3. For a planet located at $a_p = 1.2$ AU (left panels of Fig. 5), the inclination angle $i_{p\text{-out}}$ does not evolve smoothly as the inner binary decays, but suffers a jump as r_L crosses a_p , subsequently oscillating around a reference angle. Moreover, the orbital eccentricity rapidly grows until it starts oscillating around a mean value of $\langle e_p \rangle \sim 0.16$, maintaining from then on a steady-state behavior. For a planet at $a_p = 1.8$ AU (right panels), the orbital evolution is even more complex. In this case, the exponential growth in eccentricity does not saturate at a moderate value. Instead, e_p reaches values close to 1. The erratic evolution in e_p is accompanied by a similar behavior in the planet’s inclination $i_{p\text{-out}}$. Instead of oscillating around a mean (equilibrium) value, $i_{p\text{-out}}$ covers the entire range ($0^\circ, 180^\circ$). The high planet eccentricities reached in this case make it very unlikely for the planet to survive the orbital decay of the inner binary. Such high eccentricities will inevitably bring the planet too close to the inner binary, a region that is known to be unstable Holman & Wiegert (1999); Mudryk & Wu (2006). In this case, ejections from the system or physical collisions with the central stars are to be expected.

In Fig. 6, we show the initial and final inclinations (top panel), and the respective final eccentricities (bottom panel), computed for a set of values of a_p using the same stellar triple configuration of Fig. 5. As in Fig. 4, these results are shown together with the Laplace equilibrium surface solutions for the ini-

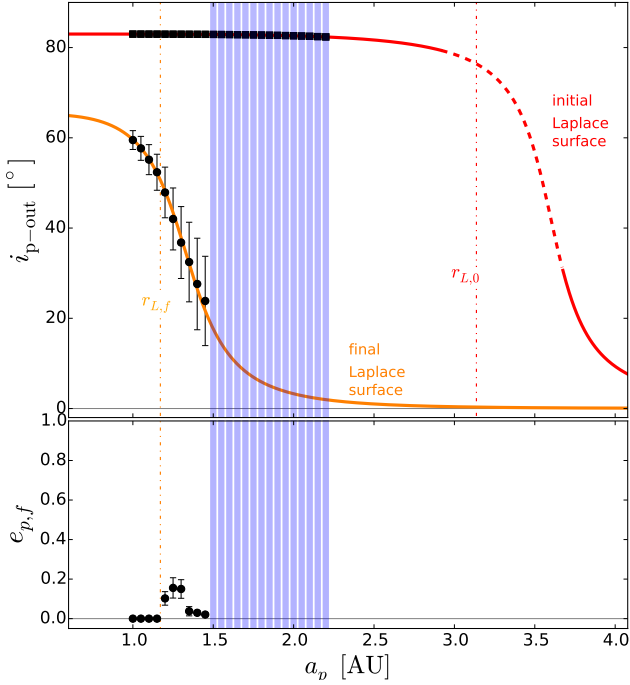


Figure 6. Top panel: similar to Fig. 4, but for the triple configuration shown in Fig. 5 ($a_{\text{in},0} = 0.3$ AU, $i_{\text{in-out},0} = 83^\circ$, $a_{\text{in},f} = 0.026$ AU, $i_{\text{in-out},f} = 65.3^\circ$). Bottom panel: the corresponding *final* eccentricity of each planet. Error bars specify the oscillation amplitude around the mean value. Purple symbols denote planet orbits that were excited into eccentric states. Wide blue bands (for $a_p \gtrsim 1.5$ AU) denote planet orbits with erratic behavior in inclination, covering the entire range $[0^\circ, 180^\circ]$, at *any* point during their evolution. Note that, for some values of a_p , planets do reach regular values in eccentricity and inclination even *after* having experienced erratic evolution during a finite period of time before binary circularization; such cases are still depicted by blue bands, since their survival is deemed unlikely (see Fig S2).

tial state ($a_{\text{in},0} = 0.3$ AU and $i_{\text{in-out},0} = 83^\circ$) and the final state ($a_{\text{in},f} = 0.026$ AU and $i_{\text{in-out},f} = 65.3^\circ$). Unlike Fig. 4, we find that, depending on a_p , planet orbits do not always stay circular, and their inclinations $i_{p\text{-out}}$ do not always land exactly on the final Laplace surface. For $a_p \lesssim r_{L,f}$, planets end up very close (on average) to the final Laplace surface (while exhibiting some minor oscillations around it), and maintain a negligible eccentricity. For $a_p \gtrsim r_{L,f}$, planets suffer a small kick in eccentricity as they cross the “transition” regime ($a_p = r_L$), and their inclinations oscillate with significant amplitude around a mean value that is close, but not necessarily equal to, the one given by Laplace equilibrium (see Fig. 5, left panel). At even larger a_p ($\gtrsim 1.5$ AU), we find that the evolution of the planet is no longer regular (see Fig. 5, right panel): both e_p and $i_{p\text{-out}}$ undergo large-amplitude, erratic variations ($e_p \simeq 0 - 1$ and $i_{p\text{-out}} \simeq 0^\circ - 180^\circ$). Indeed, for large values of a_p , the planet’s evolution is most likely chaotic, since the results depend sensitively on the initial conditions (see Supplementary Information and Fig. S2). Erratic evolution (in eccentricity and inclination) may last indefinitely or may end before circularization of the inner binary has completed, in which case planets can exit the erratic phase at a random inclination (including angles $> 90^\circ$). In either case, these planets, having experienced erratic, large-amplitude variations of e_p , are likely to be ejected from the system or to collide with the binary stars.

In the above, our calculations have ignored the mass of the circumbinary planet m_p based on the assumption that the plan-

etary mass is always much smaller than M_{in} and M_{out} . However, over secular time scales, a finite planet mass can affect the dynamics of the inner binary to the point of suppressing the eccentricity oscillations caused by the tertiary Holman et al. (1997). The planet-induced precession frequency of the binary is of order $\Omega_{\text{in-p}} \simeq n_{\text{in}} (m_p/M_{\text{in}}) (a_{\text{in}}/a_p)^3$. The condition $\Omega_{\text{in-p}} \simeq \Omega_{\text{in-out}}$ allows us to define the critical planet mass

$$m_{p,\text{crit}} \simeq 0.13 M_J \left(\frac{M_{\text{out}}}{1 M_\odot} \right) \left(\frac{a_p}{1.5 \text{ AU}} \right)^3 \left(\frac{a_{\text{out}}}{30 \text{ AU}} \right)^{-3} \quad (7)$$

(where M_J is the mass of Jupiter) above which the precession of the binary due to the planet is faster than that due to the tertiary star. For small m_p , the effects of a finite planet mass on the LK cycles are qualitatively similar to those of other short range forces Fabrycky & Tremaine (2007); Liu et al. (2015), imposing an upper limit on the maximum eccentricity of the binary. In Fig. 7 we show the maximum eccentricity achieved by the inner binary as a function of planet mass obtained from integrations of the 4-body secular system (see Supporting materials). For the example depicted in Fig. 3 ($a_p = 1.5$ AU and $m_{p,\text{crit}} \simeq 0.6 M_J$), we find that $m_p \gtrsim 1 M_J \simeq 1.7 m_{p,\text{crit}}$ is enough to substantially suppress the oscillations in e_{in} . For $m_p \lesssim 0.3 M_J \simeq 0.5 m_{p,\text{crit}}$ (about the mass of Saturn), the minimum pericenter separation of the binary $a_{\text{in},0}(1 - e_{\text{in,max}}) \approx 0.09 a_{\text{in},0}$ is only 17% larger than $0.077 a_{\text{in},0}$, the value corresponding to $m_p = 0$. Such a planet ($m_p \lesssim 0.3 M_J$) will only delay the orbital shrinkage of the inner binary, but not prevent it (see Supplementary materials for an example).

Throughout this paper, we have included only the quadrupole potential from the tertiary companion acting on the inner binary and the planet. This is a good approximation when the companion has zero orbital eccentricity. For general companion eccentricities, octupole and higher-order potentials may introduce more complex dynamical behaviors for the inner binary and for the planet (see, e.g., Ford et al. (2000); Naoz et al. (2011); Katz et al. (2011); Liu et al. (2015)). For example, in N -body calculations (which include high order terms automatically) the planet may attain a non-zero eccentricity as the inner binary decays even in the moderate inclination case (see the Supplementary material for one such example). A systematic study of these complex “high-order” effects is beyond the scope of this paper and will be the subject of future work.

DISCUSSION

We have explored the orbital evolution of planets around binaries undergoing orbital decay via the “LK+Tide” mechanism driven by distant tertiary companions. We have shown that planets may survive the orbital decay of the binary for tertiary companions at moderate initial inclinations ($i_{\text{in-out},0} \lesssim 75^\circ$). In such case, planets on circular orbits adiabatically follow an equilibrium solution as the triple system evolves, becoming misaligned with their host binary; the final misalignment angle $i_{p\text{-in}}$ is a monotonically increasing function of the binary-planet distance a_p . At higher inclinations ($i_{\text{in-out},0} \gtrsim 80^\circ$), the adiabatic evolution is broken when planets encounter an unstable equilibrium. Then the planet orbit can develop erratic behavior in eccentricity and inclination. Very eccentric circumbinary orbits may be disrupted by the inner binary via dynamical instabilities, resulting in either the ejection of the planet or its collision onto the stars. Interestingly, even in this high-inclination regime, we have found that some planets may evolve into stable, misaligned and eccentric orbits.

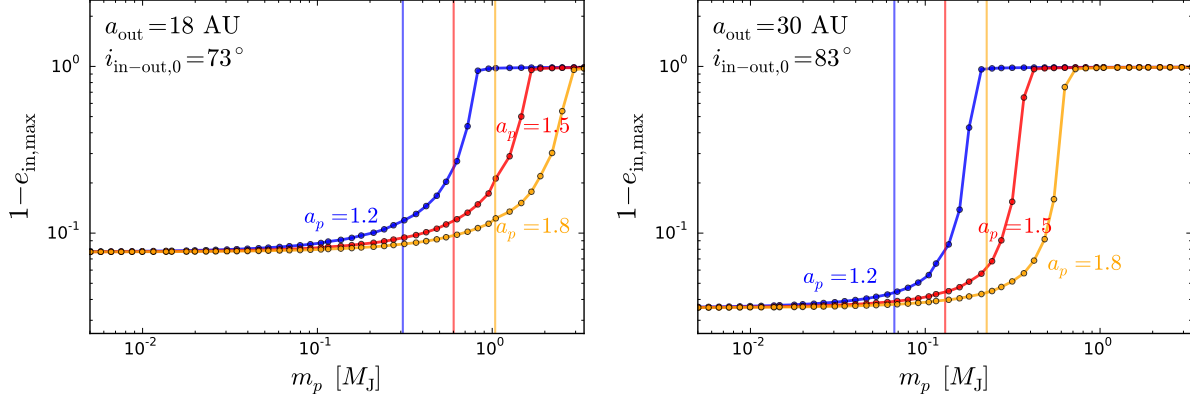


Figure 7. Left: maximum eccentricity $e_{\text{in,max}}$ of the inner binary in the triple configuration of Fig. 4 achieved during the LK cycles as a function of planet mass m_p for three different values of the planet semimajor axis a_p : 1.2 AU (blue), 1.5 AU (red) and 1.8 AU (orange). Vertical lines denote the value of $m_{p,\text{crit}}$ (Eq. 7) for each of the different values of a_p . Right: same as left panel, but for a triple configuration as in Fig. 6. In general, LK oscillations are entirely suppressed for $m_p \gtrsim 2m_{p,\text{crit}}$. For smaller planet mass ($m_p < \frac{1}{2}m_{p,\text{crit}}$), the eccentricity oscillation amplitude is only slightly modified.

In our scenario, the abundance of misaligned planets around compact binaries depends on the frequency of moderate initial inclination stellar triples relative to those with high inclinations. High inclination stellar triples may be the progenitors of the majority of compact binaries, since the very high eccentricities reached by the inner binary make orbital decay faster. Our calculations suggest that planets within such high inclination triples have less chances of survival during the inner binary’s orbital decay. The efficiency of tidal decay depends on the dissipation time scale t_V within the stars (see supplementary material). We have found that dissipation time scales of order 20 – 50 years can circularize inner binaries with $i_{\text{in-out},0} \gtrsim 78^\circ$ within a Hubble time, but if $i_{\text{in-out},0} \sim 70^\circ$, then $t_V \simeq 1 - 5$ yr is required. However, given the large parameter space in orbital configurations, and the uncertainty in realistic values of t_V (which may vary during stellar evolution), we cannot discard the possibility that some binaries, perhaps still undergoing orbital decay and circularization, may be part of moderate-inclination stellar triples, and may therefore be candidate hosts to highly misaligned planets.

An additional caveat to the abundance of misaligned circumbinary planets that is not addressed in this work concerns the likelihood of planets forming within inclined hierarchical triples with $a_{\text{out}}/a_{\text{in}} \sim 100$. Planet formation will be limited by disk truncation from inside (at $a \sim 3a_{\text{in}}$) and from outside (at $a \sim a_{\text{out}}/3$) Artymowicz & Lubow (1994); Miranda & Lai (2015). Thus, for the parameters explored in this paper, planets would be confined to form between 1 and 10 AU. In addition to disk truncation and warping Tremaine & Davis (2014), planetesimal dynamics in this systems could be affected by the tidal forcing of the inner binary and the outer companion, introducing additional complications to the formation of planetary cores Rafikov & Silsbee (2015); Silsbee & Rafikov (2015).

As noted before, currently no planets have been detected around eclipsing compact ($P_{\text{in}} \lesssim 5$ days) stellar binaries. Our work suggests that if planets are able to form within (moderately) compact triples, they are likely to survive the tidal shrinkage of the central binary, evolving into inclined orbits. The detection of these misaligned circumbinary planets may be challenging. The planets that survive the orbital decay of the binary lie close to/on the Laplace surface, which follows with the precession of the inner binary axis $\hat{\mathbf{L}}_{\text{in}}$ respect to the outer binary axis $\hat{\mathbf{L}}_{\text{out}}$. The coupled precession of the inner binary and the planet orbits will

produce short-lived “transiting windows”, but these windows appear periodically over very long time scales [of order $1/\Omega_{\text{in-out}} \sim P_{\text{in}}(a_{\text{out}}/a_{\text{in}})^3 \sim 10^5 - 10^6$ years]. An alternative detection strategy is to look for eclipse timing variations. The perturbation on the inner binary exerted by a planet of mass m_p introduces a timing signature (on the time scale of the planet’s orbital period) of the magnitude $\Delta P_{\text{in}} \sim (3/8\pi)P_{\text{in}}(m_p/M_{\text{in}})(a_{\text{in}}/a_p)^{3/2}$ Mayer (1990); Borkovits et al. (2003). For values of $m_p \sim 0.5M_J \sim 0.0005M_{\text{in}}$, $a_p \sim 1.0\text{AU}$, $a_{\text{in}} \sim 0.05\text{AU}$ and $P_{\text{in}} \sim 5$ days, the maximum eclipse timing variation is of order ~ 0.3 s, approaching the noise level for some nearby binaries, but in general, still below the detection limits for most eclipse timing detections Conroy et al. (2014). However, short cadence data with current observational capabilities might provide enough timing precision to accomplish such measurements.

We thank Sarah Ballard, Konstantin Batygin, Matthew Holman and Bin Liu for discussions and comments. We also thank the referee, Daniel Fabrycky for valuable comments and suggestions. This work has been supported in part by NSF grant AST-1211061, and NASA grants NNX14AG94G and NNX14AP31G.

Note added: During of the revision of our manuscript, we became aware of a preprint by D. Martin, T. Mazeh and D. Fabrycky, which addresses a similar issue (i.e. the dearth of planets around compact binaries) as our paper.

REFERENCES

- Armstrong D. J., Osborn H. P., Brown D. J. A., Faedi F., Gómez Maqueo Chew Y., Martin D. V., Pollacco D., Udry S., 2014, MNRAS, 444, 1873
- Artymowicz P., Lubow S. H., 1994, ApJ, 421, 651
- Beaugé C., Nesvorný D., 2012, ApJ, 751, 119
- Borkovits T., Érdi B., Forgács-Dajka E., Kovács T., 2003, A & A, 398, 1091
- Chambers J. E., 1999, MNRAS, 304, 793
- Conroy K. E., Prša A., Stassun K. G., Orosz J. A., Fabrycky D. C., Welsh W. F., 2014, AJ, 147, 45
- Doyle et al. L. R., 2011, Science, 333, 1602
- Eggleton P. P., Kiseleva L. G., Hut P., 1998, ApJ, 499, 853
- Eggleton P. P., Kiseleva-Eggleton L., 2001, ApJ, 562, 1012
- Fabrycky D., Tremaine S., 2007, ApJ, 669, 1298

- Ford E. B., Kozinsky B., Rasio F. A., 2000, *ApJ*, 535, 385
 Holman M., Touma J., Tremaine S., 1997, *Nature*, 386, 254
 Holman M. J., Wiegert P. A., 1999, *AJ*, 117, 621
 Katz B., Dong S., Malhotra R., 2011, *Physical Review Letters*, 107, 181101
 Kostov V. B., McCullough P. R., Carter J. A., Deleuil M., Díaz R. F., Fabrycky D. C., Hébrard G., Hinse T. C., Mazeh T., Orosz J. A., Tsvetanov Z. I., Welsh W. F., 2014, *ApJ*, 784, 14
 Kostov V. B., McCullough P. R., Hinse T. C., Tsvetanov Z. I., Hébrard G., Díaz R. F., Deleuil M., Valenti J. A., 2013, *ApJ*, 770, 52
 Kozai Y., 1962, *AJ*, 67, 591
 Lidov M. L., 1962, *P&SS*, 9, 719
 Liu B., Muñoz D. J., Lai D., 2015, *MNRAS*, 447, 751
 Mayer P., 1990, *Bulletin of the Astronomical Institutes of Czechoslovakia*, 41, 231
 Mazeh T., Shaham J., 1979, *A & A*, 77, 145
 Miranda R., Lai D., 2015, *ArXiv e-prints*
 Mudryk L. R., Wu Y., 2006, *ApJ*, 639, 423
 Naoz S., Farr W. M., Lithwick Y., Rasio F. A., Teyssandier J., 2011, *Nature*, 473, 187
 Orosz J. A., Welsh W. F., Carter J. A., Brugamyer E., Buchhave L. A., et al 2012, *ApJ*, 758, 87
 Orosz J. A., Welsh W. F., Carter J. A., Fabrycky D. C., Cochran W. D., et al 2012, *Science*, 337, 1511
 Rafikov R. R., Silsbee K., 2015, *ApJ*, 798, 69
 Schwamb M. E., Orosz J. A., Carter J. A., Welsh W. F., Fischer D. A., et al 2013, *ApJ*, 768, 127
 Silsbee K., Rafikov R. R., 2015, *ArXiv e-prints*
 Slawson R. W., Prša A., Welsh W. F., Orosz J. A., Rucker M., et al. 2011, *AJ*, 142, 160
 Tamayo D., Burns J. A., Hamilton D. P., Nicholson P. D., 2013, *AJ*, 145, 54
 Tokovinin A., Thomas S., Sterzik M., Udry S., 2006, *A & A*, 450, 681
 Tremaine S., Davis S. W., 2014, *MNRAS*, 441, 1408
 Tremaine S., Touma J., Namouni F., 2009, *AJ*, 137, 3706
 Welsh W. F., Orosz J. A., Carter J. A., Fabrycky D. C., Ford E. B., et al 2012, *Nature*, 481, 475
 Welsh W. F., Orosz J. A., Short D. R., Haghighipour N., Buchhave L. A., et al 2014, *ArXiv e-prints*

SUPPLEMENTARY INFORMATION

S1 Equations of Motion

Consider a binary (total mass $M_{\text{in}} = m_0 + m_1$, reduced mass $\mu_{\text{in}} = m_0 m_1 / M_{\text{in}}$ and semi-major axis a_{in}) that is a member of a hierarchical triple, in which the binary and an outer companion of mass M_{out} orbit each other with a semi-major axis $a_{\text{out}} \gg a_{\text{in}}$. The shape and orientation of the inner binary orbit are specified by the eccentricity vector \mathbf{e}_{in} and the unit vector along the binary's angular momentum direction $\hat{\mathbf{L}}_{\text{in}}$; similarly, the outer companion's orbit is specified by \mathbf{e}_{out} and $\hat{\mathbf{L}}_{\text{out}}$. A planet orbiting around the inner binary has semi-major axis a_p , eccentricity vector \mathbf{e}_p and angular momentum direction $\hat{\mathbf{L}}_p$. The perturbing potential (per unit mass) acting on the planet has contributions from the inner binary, $\langle\langle\Phi_{\text{in}}\rangle\rangle$, and from the outer companion, $\langle\langle\Phi_{\text{out}}\rangle\rangle$ where the double brackets denote time averaging over the orbital periods of the inner binary, of the outer companion and of the planet. To quadrupole order, these potentials are given by [e.g., Tremaine et al. (2009)]

$$\begin{aligned} \langle\langle\Phi_{\text{in}}\rangle\rangle = & -\frac{1}{8} \frac{\mathcal{G} M_{\text{in}}}{a_p} (1 - e_p^2)^{-3/2} \left(\frac{\mu_{\text{in}}}{M_{\text{in}}} \right) \left(\frac{a_{\text{in}}}{a_p} \right)^2 \\ & \times \left[1 - 6e_{\text{in}}^2 - 3(1 - e_{\text{in}}^2)(\hat{\mathbf{L}}_{\text{in}} \cdot \hat{\mathbf{L}}_p)^2 + 15(\mathbf{e}_{\text{in}} \cdot \hat{\mathbf{L}}_p)^2 \right], \end{aligned} \quad (\text{A1})$$

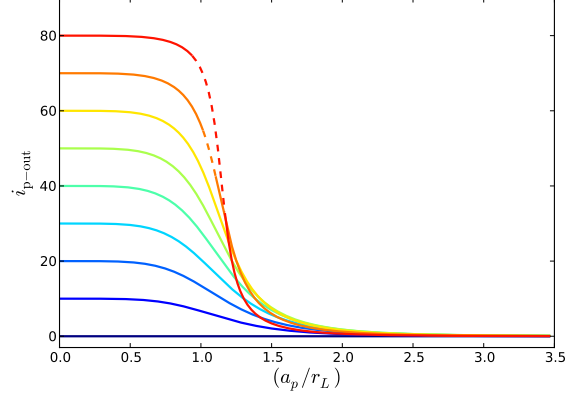


Figure A1. Classical Laplace equilibrium for a test particle in a circular orbit within a hierarchical stellar triple. The eccentricity of the inner binary is set to zero. The inner-to-outer binary inclination $i_{\text{in-out}}$ ranges from 0° (bottom blue curve) to 80° (top red curve). The dashed portion of the curve indicates unstable equilibrium,

and

$$\begin{aligned} \langle\langle\Phi_{\text{out}}\rangle\rangle = & -\frac{1}{8} \frac{\mathcal{G} M_{\text{in}}}{a_p} (1 - e_{\text{out}}^2)^{-3/2} \left(\frac{M_{\text{out}}}{M_{\text{in}}} \right) \left(\frac{a_p}{a_{\text{out}}} \right)^3 \\ & \times \left[1 - 6e_p^2 - 3(1 - e_p^2)(\hat{\mathbf{L}}_{\text{out}} \cdot \hat{\mathbf{L}}_p)^2 + 15(\hat{\mathbf{L}}_{\text{out}} \cdot \mathbf{e}_p)^2 \right]. \end{aligned} \quad (\text{A2})$$

In our actual calculations, we will set the outer orbit's eccentricity e_{out} to zero; this guarantees that higher order octupole terms of the potential $\langle\langle\Phi_{\text{out}}\rangle\rangle$ are identically zero. Similarly, setting the inner binary to have a mass ratio of unity (which means that $\mu_{\text{in}}/M_{\text{in}} = 1/4$) makes the octupole terms of the inner potential $\langle\langle\Phi_{\text{in}}\rangle\rangle$ vanish. Therefore, the quadrupole potentials given above capture the secular dynamics to high accuracy.

From the potentials $\langle\langle\Phi_{\text{in}}\rangle\rangle$ and $\langle\langle\Phi_{\text{out}}\rangle\rangle$, we can derive equations of motion for the dimensionless angular momentum vector of the planet, $\mathbf{j}_p = \sqrt{1 - e_p^2} \hat{\mathbf{L}}_p$, and the eccentricity vector \mathbf{e}_p [see Tremaine et al. (2009); Liu et al. (2015)]:

$$\begin{aligned} \frac{d\mathbf{j}_p}{dt} = & n_p \left\{ \frac{3}{2} \frac{\epsilon_{\text{in}}}{(1 - e_p^2)^{5/2}} \left[(1 - e_{\text{in}}^2)(\hat{\mathbf{L}}_{\text{in}} \cdot \mathbf{j}_p)(\mathbf{j}_p \times \hat{\mathbf{L}}_{\text{in}}) \right. \right. \\ & \left. \left. - 5(\mathbf{e}_{\text{in}} \cdot \mathbf{j}_p)(\mathbf{j}_p \times \mathbf{e}_{\text{in}}) \right] \right. \\ & \left. + \frac{3}{4} \epsilon_{\text{out}} \left[(\mathbf{j}_p \cdot \hat{\mathbf{L}}_{\text{out}})(\mathbf{j}_p \times \hat{\mathbf{L}}_{\text{out}}) - 5(\mathbf{e}_p \cdot \hat{\mathbf{L}}_{\text{out}})(\mathbf{e}_p \times \hat{\mathbf{L}}_{\text{out}}) \right] \right\}, \end{aligned} \quad (\text{A3a})$$

and

$$\begin{aligned} \frac{d\mathbf{e}_p}{dt} = & n_p \left\{ \frac{3}{2} \frac{\epsilon_{\text{in}}}{(1 - e_p^2)^{5/2}} \left[(1 - e_{\text{in}}^2)(\hat{\mathbf{L}}_{\text{in}} \cdot \mathbf{j}_p)(\mathbf{e}_p \times \hat{\mathbf{L}}_{\text{in}}) \right. \right. \\ & \left. \left. - 5(\mathbf{e}_{\text{in}} \cdot \mathbf{j}_p)(\mathbf{e}_p \times \mathbf{e}_{\text{in}}) \right] \right. \\ & - \frac{3}{4} \frac{\epsilon_{\text{in}}}{(1 - e_p^2)^{7/2}} \left[(1 - 6e_{\text{in}}^2)(1 - e_p^2) + 25(\mathbf{e}_{\text{in}} \cdot \mathbf{j}_p)^2 \right. \\ & \left. - 5(1 - e_{\text{in}}^2)(\hat{\mathbf{L}}_{\text{in}} \cdot \mathbf{j}_p)^2 \right] \mathbf{j}_p \times \mathbf{e}_p \\ & \left. + \frac{3}{4} \epsilon_{\text{out}} \left[(\mathbf{j}_p \cdot \hat{\mathbf{L}}_{\text{out}})(\mathbf{e}_p \times \hat{\mathbf{L}}_{\text{out}}) + 2\mathbf{j}_p \times \mathbf{e}_p \right. \right. \\ & \left. \left. - 5(\mathbf{e}_p \cdot \hat{\mathbf{L}}_{\text{out}})(\mathbf{j}_p \times \hat{\mathbf{L}}_{\text{out}}) \right] \right\}, \end{aligned} \quad (\text{A3b})$$

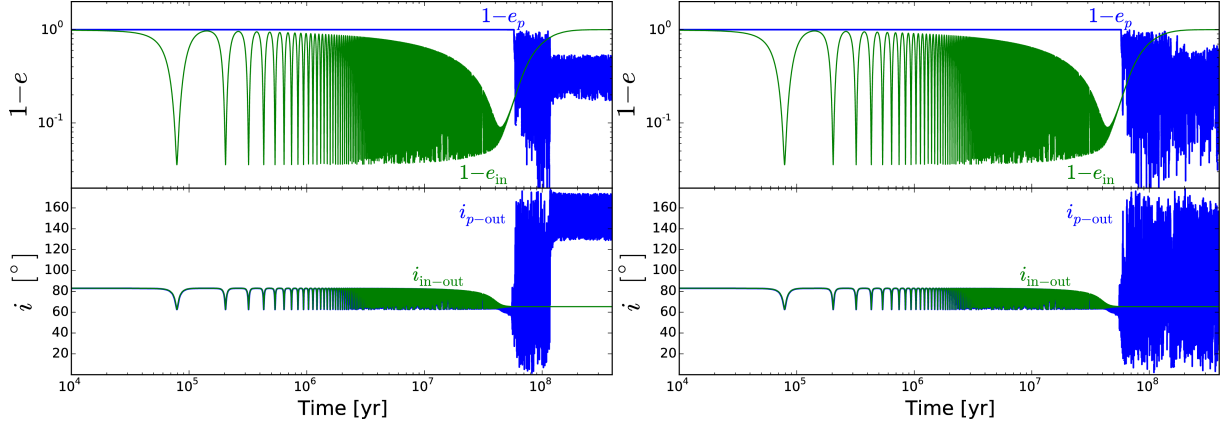


Figure A2. Two examples of planet orbital evolution with nearly identical initial conditions showing very different outcomes. As in Fig. 5 in the main text, the triple system parameters are $a_{\text{in},0} = 0.3$ AU, $a_{\text{out}} = 30$ AU and $i_{\text{in-out},0} = 83^\circ$. The left panels show the eccentricity and inclination evolution of the planet (blue) and inner binary (green) when $a_p = 1.6000$ AU. The right panels show the same quantities (the evolution of the inner binary is identical in both cases) for a planet with $a_p = 1.6002$ AU. The dramatic difference between the two outcomes of the planet’s eccentricity and inclination indicates the chaotic nature of planetary orbits undergoing erratic evolution for high-inclination stellar triples.

where we have introduced the dimensionless quantities

$$\epsilon_{\text{in}} \equiv \frac{1}{2} \left(\frac{\mu_{\text{in}}}{M_{\text{in}}} \right) \left(\frac{a_{\text{in}}}{a_p} \right)^2, \quad (\text{A4a})$$

$$\epsilon_{\text{out}} \equiv \frac{1}{(1 - e_{\text{out}}^2)^{3/2}} \left(\frac{M_{\text{out}}}{M_{\text{in}}} \right) \left(\frac{a_p}{a_{\text{out}}} \right)^3. \quad (\text{A4b})$$

Note that, in the notation of the main body of this article $\Omega_{p-\text{in}} = n_p \epsilon_{\text{in}}$ and $\Omega_{p-\text{out}} = n_p \epsilon_{\text{out}}$.

By setting $d\mathbf{j}_p/dt = d\mathbf{e}_p/dt = 0$ we obtain the equilibrium solution for the planet’s orbit under the influence of both inner and outer torques. This is known as “classical Laplace equilibrium” in the special case of $e_{\text{in}} = 0$ Tremaine et al. (2009); Tamayo et al. (2013). From Eq. (A3a), and setting $e_{\text{in}} = 0$, the equation for coplanar Laplace equilibrium reads:

$$0 = 2\epsilon_{\text{in}} (\hat{\mathbf{L}}_{\text{in}} \cdot \mathbf{j}) (\mathbf{j} \times \hat{\mathbf{L}}_{\text{in}}) + \epsilon_{\text{out}} (\mathbf{j} \cdot \hat{\mathbf{L}}_{\text{out}}) (\mathbf{j} \times \hat{\mathbf{L}}_{\text{out}}). \quad (\text{A5})$$

Using orbital elements, we can write this expression as Tremaine et al. (2009); Tamayo et al. (2013)

$$0 = 2\epsilon_{\text{in}} \sin 2(i_{p-\text{out}} - i_{\text{in-out}}) + \epsilon_{\text{out}} \cos 2i_{p-\text{out}}. \quad (\text{A6})$$

We can solve this transcendental equation for $i_{p-\text{out}}$ as a function of the ratio $\epsilon_{\text{out}}/\epsilon_{\text{in}}$, or equivalently, as a function of the Laplace radius r_L (see Eq. 5 in the main body of this article), since $(r_L/a_p)^5 = \epsilon_{\text{in}}/\epsilon_{\text{out}}$. Fig. A1 shows the Laplace surface solution as a function of r_L/a_p for different values of $i_{\text{in-out}}$ ranging from 0° to 90° . This solution of the classical Laplace surface is used in Figures 4 and 5 of the main body of the article.

In our numerical calculations, we directly integrate Eqs. A3 together with the evolution equations of the hierarchical triple as the inner binary undergoes LK oscillations with tidal dissipation. In principle, this system consists of 24 coupled differential equations (involving the vectors \mathbf{j}_{in} , \mathbf{e}_{in} , \mathbf{j}_p , \mathbf{e}_p , \mathbf{j}_{out} , \mathbf{e}_{out} for the orbits, and the spin vectors $\boldsymbol{\Omega}_0$ and $\boldsymbol{\Omega}_1$ for each of the two central stars). We have simplified this system as follows: neglect the evolution of the outer orbit (valid approximation when the outer angular momentum dominates); include only short range forces acting on the secondary central star (i.e. the primary star is a non-spinning “rigid sphere”); assume pseudo-synchronization [e.g., (16)] and orbital alignment for the spin vector $\boldsymbol{\Omega}_1$. This simplification reduces

the number of equations to 12, while still capturing all the essential physics of the problem.

For the evolution of the vectors \mathbf{e}_{in} and $\hat{\mathbf{L}}_{\text{in}} = \mathbf{j}_{\text{in}}/|\mathbf{j}_{\text{in}}|$, we use the formalism of Eggleton & Kiseleva-Eggleton (2001) and Fabrycky & Tremaine (2007):

$$\frac{d\mathbf{j}_{\text{in}}}{dt} = \frac{d\mathbf{j}_{\text{in}}}{dt} \Big|_{\text{in-out}} + \frac{d\mathbf{j}_{\text{in}}}{dt} \Big|_{\text{SRF}} \quad (\text{A7a})$$

$$\frac{d\mathbf{e}_{\text{in}}}{dt} = \frac{d\mathbf{e}_{\text{in}}}{dt} \Big|_{\text{in-out}} + \frac{d\mathbf{e}_{\text{in}}}{dt} \Big|_{\text{SRF}} \quad (\text{A7b})$$

where the first terms on the right hand side correspond to the conservative tidal effect of the tertiary and the second terms to the conservative and non-conservative short range forces. In $d\mathbf{j}_{\text{in}}/dt|_{\text{SRF}}$ and $d\mathbf{e}_{\text{in}}/dt|_{\text{SRF}}$, an important parameter is the viscous time t_V associated with the dissipation within the stars. This parameter is the main source of uncertainty in our calculations. We vary t_V between ~ 1 year to 55 years [the value used by Fabrycky & Tremaine (2007)]. Note that we include dissipation only within one of the stars. The effective tidal quality factor Q scales proportionally with t_V as Eggleton & Kiseleva-Eggleton (2001):

$$Q = \frac{4}{3} \frac{k}{(1+2k)^2} \frac{Gm_1}{R_{*,1}^3} \frac{t_V}{n_{\text{in}}}, \quad (\text{A8})$$

where we use $m_1 = m_0 = 0.5M_\odot$, $R_{*,1} = R_{*,0} = 0.5R_\odot$ and k (the classical apsidal motion constant) is set to 0.014. We see that one to two orders of magnitude of variation in t_V is not unreasonable, given the large degree of uncertainty in the tidal Q values for different types of stars. The assumption of pseudo-synchronization and spin-orbit alignment also introduces uncertainties, although the dominant uncertainty still lies in the value of t_V . These uncertainties ultimately affect not the final, circularized orbit of the inner binary, but how fast this final state can be reached (see the discussion in the main body of the text).

S2 Erratic evolution and chaotic behavior

In Fig. A2 we show two integrations for planets within the stellar triple configuration of Fig. 6 in the main text. The left panels show the eccentricity and inclination evolution of a planet with $a_p = 1.6$ AU, and the right panels show the same for a planet with $a_p = 1.6002$ (about a 0.1% difference in semi-major axis). The

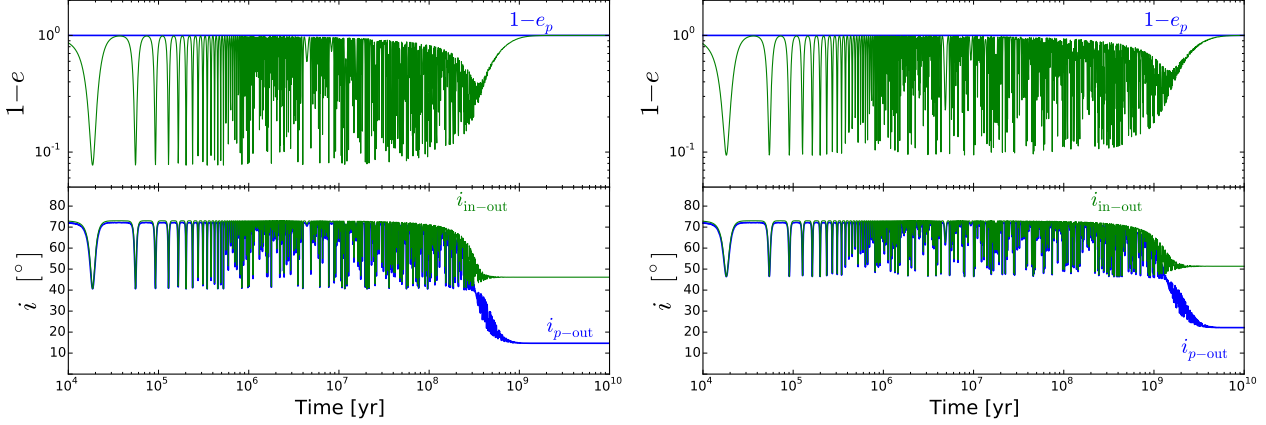


Figure A3. Effects of planet mass on the orbital evolution of the inner binary and the planet. Left: Orbital evolution of a binary ($a_{\text{in},0} = 0.3$ AU) and a circumbinary planet ($a_p = 1.5$ AU) in a triple with $i_{\text{in-out},0} = 73^\circ$ and $a_{\text{out}} = 18$ AU where $m_0 + m_1 = M_{\text{in}} = M_{\text{out}} = 1M_\odot$ and $m_p = 1$ Earth mass. The circularization of the inner binary takes place at the same rate as the case with $m_p = 0$. Right: Same as the left panel, but with $m_p = 1$ Saturn mass. Circularization is not prevented, but it takes ~ 4 times longer than the $m_p = 0$ case.

evolution of both planets is identical until circular orbits become unstable, at which point rapid eccentricity growth is triggered, followed by highly erratic behavior in the evolution of e_p and $i_{p\text{-out}}$. The first example “exits” the erratic region and finds a stationary state in which e_p and $i_{p\text{-out}}$ oscillate around a well-defined value with constant amplitude (in this case, the planet lands on a retrograde orbit respect to $\hat{\mathbf{L}}_{\text{out}}$). However, the second example never finds “a way out” of the erratic region (which must happen before the inner binary circularizes, “locking” the properties of the system). Since both these examples go through a phase of extreme eccentricities, they are both likely to be ejected by interactions with the inner binary, and thus their chances of surviving for a long period of time are equally small, regardless of the duration of the erratic phase.

S3 Effect of finite planet mass

In the calculations above, the mass of the planet m_p has been neglected. However, the effect of finite planet mass on the inner binary can be taken into account in a self-consistent fashion by including the tidal potential on the inner binary due to the planet, which introduces the additional terms $d\mathbf{j}_{\text{in}}/dt|_{\text{in-p}}$ and $de_{\text{in}}/dt|_{\text{in-p}}$ to Eq. A7. These extra terms have the same functional form as the terms arising from the tidal potential of the tertiary $d\mathbf{j}_{\text{in}}/dt|_{\text{in-out}}$ and $de_{\text{in}}/dt|_{\text{in-out}}$. Fig. A3 depicts a similar example to that of Fig. 3, this time including the effects of $m_p \neq 0$. For a planet of 1 Earth mass, the results are indistinguishable from the test-particle case. However, for a planet of 1 Saturn mass, the effects of the modified maximum binary eccentricity (see Fig. 7) can be readily seen in the efficiency at which the binary shrinks.

S4 Example of an N -body integration

Although long-term direct N -body integrations are computationally costly, one can combine them with the output of the secular solutions to study the detailed behavior of the planetary orbit as the binary decays. Fig. A4 shows the N -body result of a dissipative binary performed using the MERCURY code Chambers (1999). We have added short range forces following Beaugé & Nesvorný (2012), including stellar tides, GR and tidal dissipation. This integration is started once the binary has undergone appreciable orbital

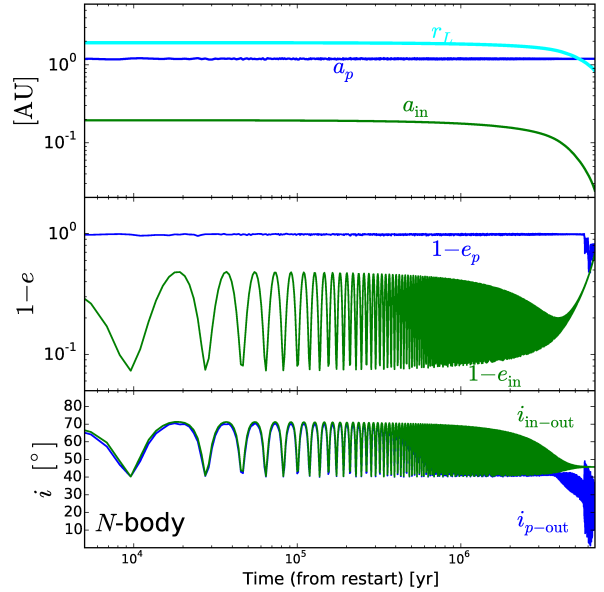


Figure A4. Example of a dissipative N -body integration of a 4-body system. Masses of the binary and companion are $m_0 = m_1 = 0.5M_\odot$ and $M_{\text{out}} = 1M_\odot$. The companion semimajor axis is $a_{\text{out}} = 18$ AU and its eccentricity is 0.2. The planet semimajor axis is $a_p = 1.2$ AU and its mass is zero. The N -body integration is started once the binary has undergone appreciable orbital decay, when $a_{\text{in}} = 0.19$ AU, $e_{\text{in}} = 0.516$ and $i_{\text{in-out}} = 73^\circ$. The line types are the same as in Fig. 3.

decay, but before the planet has crossed the Laplace radius r_L ; the initial condition is obtained using the results of our secular calculation. In our example, the orbital evolution has been accelerated by increasing the tidal dissipation rate.

As seen from Fig. A4, before crossing the Laplace radius, the planet’s inclination adiabatically follows that of the inner binary while maintaining zero eccentricity, in full agreement with our secular results. After a_p crosses r_L , the planet develops a modest eccentricity and its inclination decouples from that of the binary. Note that since the tertiary companion has a finite eccentricity (0.2) in this example, the octupole potential on the planet likely plays an important role. This may explain the development of finite planet eccentricity for a system with such a modest $i_{\text{in-out}}$.